applied sciences

MDPI

Article

Solderability Tests Toward Miniaturized Microelectronics: Applicability and Limitations of Micro-Wetting Balance Testing of SnAgCu and SnBi Solders

Cham Thi Trinh * and Steffen Wiese

Chair of Microintegration and Reliability, Faculty of Natural Sciences and Technology, Saarland University, 66123 Saarbrucken, Germany; s.wiese@mx.uni-saarland.de

* Correspondence: thi.trinh@uni-saarland.de; Tel.: +49-681-302-71823

Abstract

This study presents a comprehensive investigation of the micro-wetting behavior of SAC305 and SnBi58 solders on chip components. Micro-wetting balance tests, which employ small solder globules, enable direct evaluation of solder wettability on miniature electronic components such as 1206 chip resistors and 1206 and 0603 chip capacitors. Unlike conventional wetting tests that use large solder baths, the micro-wetting method suppresses excessive solder rise, making it suitable for testing small-scale components. The results demonstrate that micro-wetting testing is a reliable method for evaluating solder wettability on chip components when appropriate globule size, test temperature, and experimental parameters such as immersion depth and speed are carefully controlled. Among the tested conditions, 2 mm diameter solder globules are identified as the optimal choice because they offer improved thermal management and reduced surface oxidation. The wetting times measured for SnBi58 are comparable to those obtained for conventional SAC305 solder, whereas the maximum wetting forces are generally lower. However, micro-wetting curves exhibit noticeable fluctuations, which complicate the analysis of additional parameters, such as maximum wetting force and wetting rate, and limit direct comparison with standard reference values.

Keywords: solderability; micro-wetting balance test; SnAgCu; SnBi58; miniaturization; globule test; chip components

Academic Editors: Fariba Malekpour Galogahi, Haotian Cha and Jun Zhang

Received: 28 November 2025
Revised: 19 December 2025
Accepted: 22 December 2025
Published: 7 January 2026

1. Introduction

The growing demand for higher functionality and performance of electronic devices has made miniaturization a key driving force in the development of modern, innovative electronic technology, enabling the creation of smaller, lighter, and more powerful electronic systems. As device dimensions shrink, interconnection technologies become critical to system performance and require meticulous design [1]. In solder-based interconnections such as surface-mount technology (SMT), ball grid arrays (BGA), and chip-scale packages (CSP), the solder material and the appropriate solder volume are key parameters governing joint quality and reliability [2–4]. Critical challenges for miniaturization are increased risks of soldering-related issues arising from inconsistencies between self-alignment forces and stand-off height [5,6] as well as the degradation of the joint reliability due to high current and temperature at the solder joints [7,8]. With the development of 3D packaging, where the size of the micro-bump is currently 25 µm and may decrease to 10 µm in the

future [9], the problem becomes even more severe due to the high volume ratio of the ongoing brittle intermetallic phases at the solder/component interface and the solder joint itself [10]. For SMT, manufacturing challenges are also related to stencil for small volume solder paste which requires the compromise between the features of printer and solder paste flux chemistry, especially for small component sizes of 01005 (400 μm × 200 μm) and 0201 (600 μm × 300 μm) [11]. In the pursuit of miniaturization, low temperature soldering plays an important role, since it can contribute to mitigate warpage defects and significantly reduce energy costs [12,13]. To comply with EU's restriction of hazardous substances (RoHS) directive and to enable miniaturization trend, Lee et al. has defined the critical requirements for lead-free solder alloys and fluxes to ensure solderability of the solder and long-term stability of the joints [4]. Among them, slow wetting spread and speed are mostly challenging since miniaturization often results in a poor wetting or vulnerability toward tombstone and voiding [14]. Additionally, evaluating system performance and assessing failures become increasingly complex as electronic components become smaller. It is often difficult to determine whether a failure originates from the device itself or from the bonding joints, as inaccurate component placement on the solder can lead to misleading failure indications. These complexities underscore the need for an effective and reliable methodology to assess the wetting behavior of solder, especially low-temperature solder alloys, on small electronic components toward miniaturized electronic devices.

The process of wetting means the spreading of the solder over metallic surfaces and forming a metallurgical bond with a metal. There are some factors affecting the wettability of solder such as the thermal demand of the systems, properties of the flux, viscosity of the solder, and chemical reactions at the interface between solder and substrates or components [15–17]. The common methods to evaluate wettability include wetting spreading test, direct contact angle measurement, and wetting balance test (WBT). The first two methods have technical limitations as it comes to very small dimensions of solder volumes since they rely on observation using microscopy or optical imaging [15,17]. The WBT is widely used since it is a fast and highly precise test which provides comprehensive data about wetting performance and can be used to test various types of components with different surface finishes. In this method, wettability is evaluated by analysis of the wetting force–time curve, which is recorded during immersion and withdrawal of the component in molten solder. The WBT using solder bath offers an easy and reproducible method, providing a preferable approach for evaluating the wettability for solders on various specimens such as printed circuit board (PCB) pad, Cu, and Ni strips [14,16,18–21]. However, this approach is not suitable to test small components due to the possibility of over-wetting as molten solder rises over the size of the components. Table 1 indicates the theoretical maximum solder rise on the surface with perfect wetting or good wetting with the typical contact angle of 40° of some common solders [22]. The data was calculated following equations in the literature [23]. The smallest heights raised are for SnBi58 and still much larger than the dimensions of metallic parts of components. To overcome this limitation, WBT using small globules (so-called micro-wetting tests) has been developed. In this approach, the small solder volumes available and the curve solder surface suppresses significantly the rise of solder on the component [23–25]. Therefore, this approach enables testing of various component sizes and types through the control of globule diameter. Additionally, the use of smaller solder volumes allows the method to more accurately reflect the actual wettability of solder during soldering process. However, this approach also faces several challenges, mainly related to sample positioning and the limited heat transfer between the small solder volume of solder and components, or oxidation surface treatments, which affect wetting kinetics and reproducibility of results [26]. So far, there are only a few reports available on WBTs for small components using solder globules, and most

of these studies date back several decades and made use of SnPb60 solders [23,27,28]. Recent works have primarily focused on evaluation of the solderability on different board finishes, or Cu and Ni strips for SAC [29,30] or SnCu0.7Ni0.05 [31,32] solder alloys, or assessment of solder paste for solar cells [33]. Nevertheless, systematic studies addressing the micro-wetting behavior directly on miniature chip components remain limited. To address this gap, this work provides a comprehensive investigation of micro-wetting behavior on chip components, focusing on the influence of varying testing conditions—including positioning configuration, globule size, and temperature—on wettability. This research is one of the first systematic studies of lead-free micro-wetting on real chip components (chip resistors and capacitors) with quantitative comparison to conventional bath results. Toward the miniaturization applications, two solder alloys are examined: (1) SAC305, a conventional solder alloy widely used in standard lead-free soldering processes; (2) SnBi58, a potential solder candidate for low temperature soldering. Accordingly, the applicability and limitations of this method for miniaturization-oriented solderability assessment will be discussed.

Table 1. The raised height for some typical solders with perfect or good wetting.

Solder	Surface Tension (mN/m)	Density (kg/m^3)	Solder Rise (mm)	
			0°	40°
SnBi58	319	8740	2.73	1.63
SnZn9	518	7270	3.81	2.28
SnPb60	417	8900	3.09	1.85
SnAg3.5	431	7390	3.45	2.06
SnCu0.7	491	7290	3.71	2.22
SnSb5	468	7250	3.63	2.17

2. Materials and Methods

The micro-wetting tests were conducted using the wetting balance tester LBT 210 (Microtronic GmbH, Neumarkt-Sankt Veit, Germany). The image of the tester is shown in Figure 1. The system enables tests with both a globule module and a bath module. The latter module contains a cylindrical solder bath with a diameter of 83 mm and a depth of 40 mm, which is able to accommodate approx. 1 kg of solder. In contrast, the globule module accommodates very tiny solder spheres with a diameter between 1 mm and 4 mm, corresponding to a mass of 3 mg . . . 200 mg of solder.

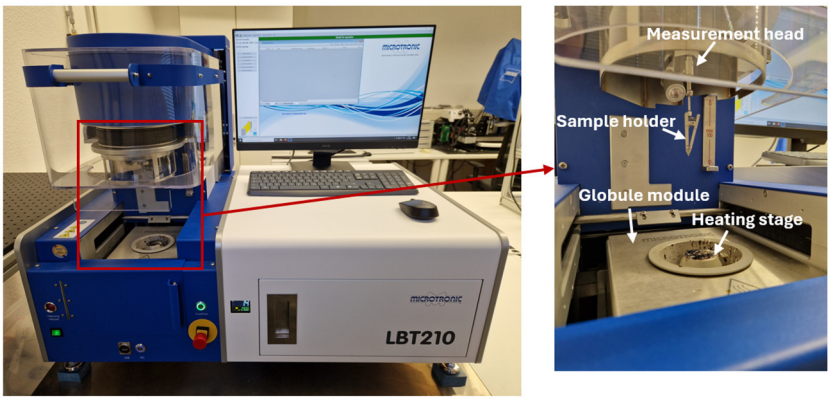

Figure 1. LBT210 solderability tester. The globule module is inserted.

Different types of specimens were used to perform wetting experiments on both modules. The specimens are subdivided into two categories. There are model-type specimens in the form of Cu-stripes to understand the general behavior of the two types of wetting tests, and component-type specimens in the form of surface-mount device (SMD) multilayer ceramic capacitors (MLCC) and SMD resistors in order to understand the wetting behavior on real component metallization. Table 2 gives an overview of specimens for the different tests and specifies the number of specimens that were used for each variation in the test. Figure 2 displays the specimens used in this study.

Table 2. Summary of the specimens that were used for the wetting experiments.

Specimen	Type	Solder Bath	Globule Module	
			2 mm	4 mm
Cu Strips	1.5 × 10 × 0.15 (W × L × T) in mm	17	0	21
CR 1206	CRCW12060000Z0EA Lead-free-Termination	0	21	54
MLCC 1206	VJ1206Y104KXACW1BC Cu/Ni/Sn(matt)-Terminals	0	10	23
MLCC 0603	CL10B104KB8NNNC Cu/Sn(100%)-Terminals	0	13	0

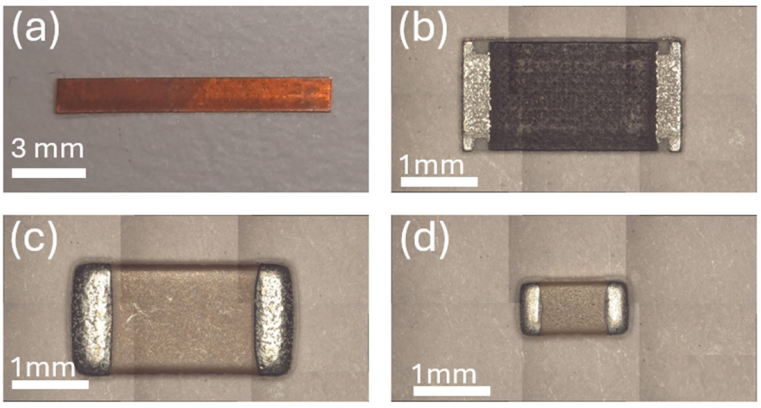

Figure 2. Images of specimens used in this study: (**a**) Cu strip; (**b**) 1206 chip resistor; (**c**) 1206 chip capacitor; (**d**) 0603 chip capacitor.

All tests were conducted using MI-T-TESTFLUX-2-50 (Microtronic GmbH) flux, a pure rosin-based, halide-activated product developed for wetting test applications. The flux was confirmed to meet the requirement of IEC 60068-2-20 [34], IPC J-STD-002 [35], IPC J-STD-003 [36] standards in relation to solderability testing. The materials and parameters used for the wetting tests in this study are summarized in Table 3.

Figure 3 shows the workflow of the wetting experiments for both cases. In order to prepare the specimens for the test, they were dipped into flux for 10 s before they are mounted to the measuring head of the LBT210 solderability tester. For the micro-wetting tests using the globule module, two droplets of the flux were applied on the solder sphere surface to remove the oxides from the globule surface, so that the micro-solder-depot is able to form an ideal globular shape. In case of the solder bath test, the oxide is removed mechanically by a scraper that slides over bath surface short before the beginning of the test. Therefore, no additional flux is needed for the solder bath test.

Table 3. Summary of the tests and specific parameters that were used for the different specimens.

Parameter		Value	
		Micro-Wetting Tests	**Conventional Bath Tests**
Test Equipment		LBT 210 solderability tester LBT-GLOBULE module	LBT 210 solderability tester LBT-BATH module
Solder	SAC305	15 mg or 2 mm-diameter globules 200 mg or 4 mm-diameter globules	approx. 1 kg of solder in the bath pot, diameter = 83 mm, depth = 40 mm
	SnBi58	200 mg or 4 mm-diameter	-
Immersion depth		0.5 mm for 4 mm-diameter 0.2 mm for 2 mm-diameter	0.5 mm, 1 mm
Immersion speed		1 mm/s	1 mm/s
Dwell time		10 s	10 s
Temperature	SAC305	245, 290 °C	245 °C
	SnBi58	160 °C	-
Flux		MI-T-TESTFLUX-2-50 Halide 0.5% (*w*/*w*), colophony content 25%	MI-T-TESTFLUX-2-50 Halide 0.5% (*w*/*w*), colophony content 25%
Components/specimens		Cu strips (0.15 × 1.5 × 15 mm) 1206 chip resistors 1206 and 0603 chip capacitors	Cu strips (0.15 × 1.5 × 15 mm)

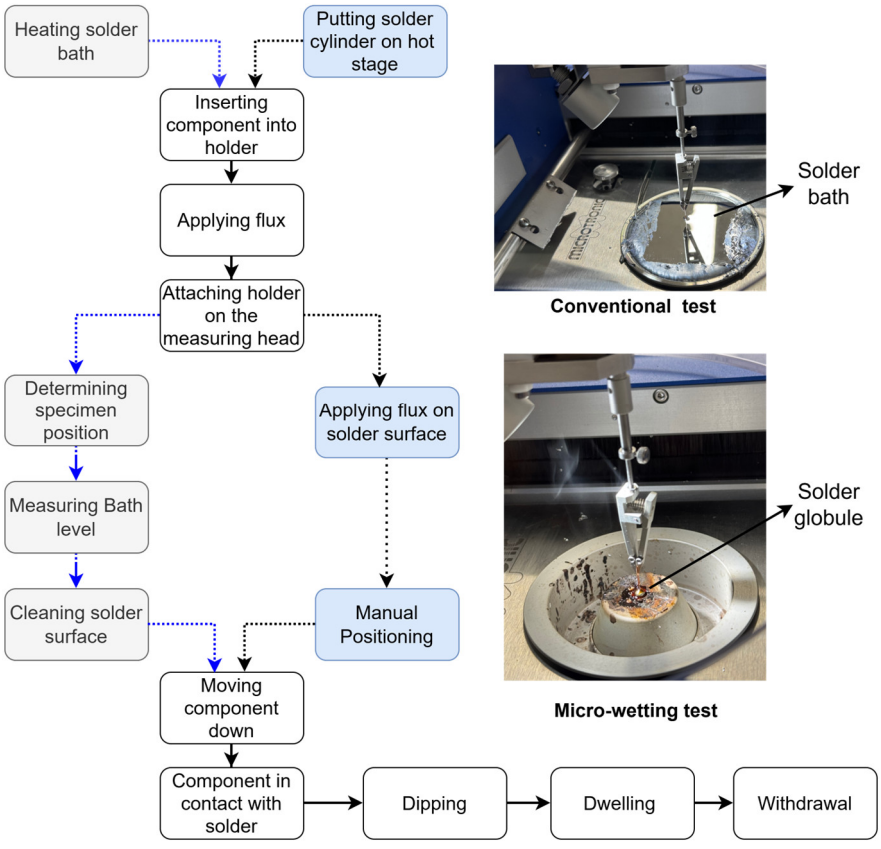

Figure 3. Workflow of the wetting experiments for use with the solder bath module (conventional test; **top right**) and the globule module (micro-wetting test; **bottom right**).

The solder bath test is highly automatized, which includes a laser triangulation measurement of the level of the liquid solder surface to determine its precise z-position relative to the specimen's lower boundary. It is impossible to provide this grade of automatization to the micro-wetting globule test, where many steps need to be carried out manually. For each test, the old solder sphere needs to be removed from the globule module, and a new one needs to be applied on it. After that, the specimen is aligned manually to the solder sphere in order to provide a centered dip into the small volume of the sphere (see Figure 4a). When these manual steps (sphere replacement, positioning, flux application) are completed, all subsequent experimental procedures are carried out automatically by the solderability tester. The immersion depth is measured by z-movement of the specimen. The surface position of the sphere is determined through the force signal, which is continuously recorded during the experiment. After the test is completed, the recorded displacement and force data is processed by the solderability tester in order to determine the contact point of the specimen with the liquid solder surface. The contact point is set to be the origin of force vs. time plot, which is provided as the result of the experiments. A typical wetting curve with features of meniscus rise for the case of the micro-wetting test is shown in Figure 5.

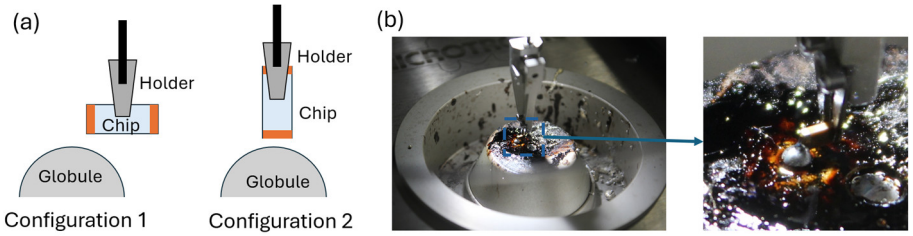

Figure 4. (**a**) Two configurations for the micro-wetting tests. (**b**) Images of micro-wetting test for a 1206 capacitor in configuration 1. The globule diameter is 4 mm.

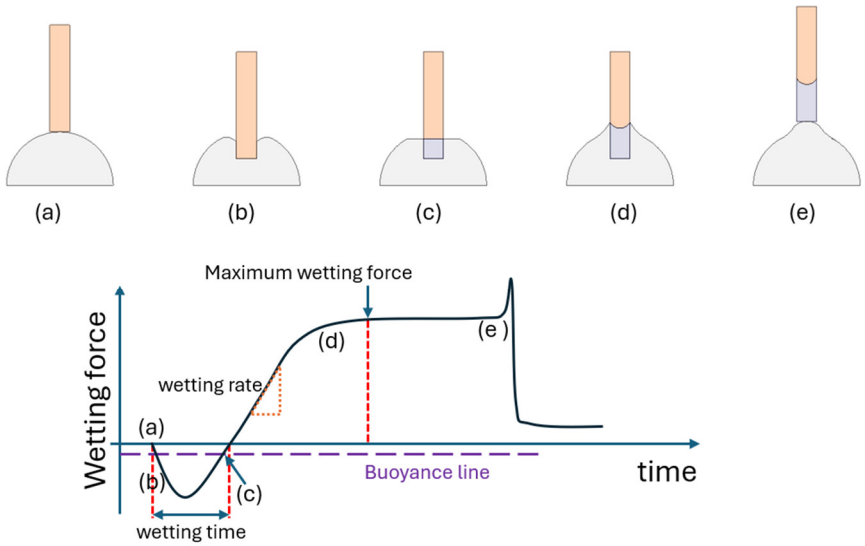

Figure 5. A typical wetting curve with features of meniscus rise for the case of micro-wetting test and important parameters from the curve. Orange, gray, and purple represent testing specimen, globule, and solder raising on specimen surface, respectively.

The following aspects are examined in this study: (1) a comparison between micro-wetting tests and conventional wetting tests; (2) the influence of positioning configuration on micro-wetting behavior; and (3) the impact of measurement conditions, including temperature, globular diameter, and variations in chip components. Table 4 summarizes the test matrix and the corresponding parameter variations in this study. The total number of tests and the number of successful tests are also displayed.

Table 4. Test matrix and variations (x denotes nothing applied).

Investigation	Section	Specimens	Variation						ΣN	N_s
			Module	Solder	Temp. (°C)	Depth (mm)	Speed (mm/s)	Conf.		
Comparison of micro-wetting tests and conventional tests	Section 3.1	Cu strips	bath	SAC305	245	0.5	1	x	11	11
			bath	SAC305	245	1	1	x	6	6
			4 mm globules	SAC305	245	0.5	1	x	11	11
			4 mm globules	SAC305	245	1	1	x	10	10
Micro-wetting tests for 1206 chip resistors: Impact of positioning configuration	Section 3.2.1	CR 1206	4 mm globules	SAC305	245	0.2	1	1	12	7
			4 mm globules	SAC305	245	0.2	1	2	9	6
Micro-wetting tests for 1206 chip resistors: Impact of Immersion depth and speed	Section 3.2.2	CR 1206	4 mm globules	SAC305	245	0.2	0.5	1	10	5
Micro-wetting tests for 1206 chip resistors: Impact of temperature and globule diameter	Section 3.2.3	CR 1206	2 mm globules	SAC305	245	0.2	1	1	10	8
			4 mm globules	SAC305	245	0.5	1	1	9	6
			2 mm globules	SAC305	290	0.2	1	1	11	8
			4 mm globules	SAC305	290	0.5	1	1	14	5
Impact of globule diameter on micro-wetting tests for 1206 chip capacitors	Section 3.3.1	MLCC 1206	2 mm globules	SAC305	245	0.2	1	1	10	7
			4 mm globules	SAC305	245	0.5	1	1	14	9
Impact of temperatures on micro-wetting tests for 0603 chip capacitors	Section 3.3.2	MLCC 0603	2 mm globules	SAC305	245	0.2	1	1	7	5
			2 mm globules	SAC305	290	0.2	1	1	6	4
Wetting behavior of SnBi58	Section 3.4	MLCC 1206	4 mm globules	SnBi58	160	0.5	1	1	9	6
Sum									159	114

Temp. = Temperature; Conf. = configuration, ΣN: total number of tests for each condition, N_s: Number of successful tests.

There are two possible configurations that can be used in micro-wetting tests, as shown in Figure 4a. Configuration 1 allows molten solders to climb vertically in all metal surfaces of the chips, while for the configuration 2, the vertical rise of solders is limited by the height of metal. For configuration 2, the climb of solders on the surface in the direction parallel to the globule depends on the immersion depth of component into the globule. For example, when a 1206 chip resistor with a length of 1.6 mm is tested, the immersion depth needs to be larger than 0.17 mm to the bellowing surface totally in 4 mm-diameter globules. To satisfy this requirement while preventing solder from climbing over the metal part, the immersion depth of 0.2 mm was chosen for this configuration. Practically, configuration 2 is easier to implement in experimental setups, such as inserting components into the holder, positioning the components, or applying flux, and the results will be expected to be more reproducible.

To provide an overview of the experimental outcomes, all wetting curves, including both successful and failed tests, were plotted. A test is classified as failed if the corresponding wetting curve exhibited one or more of the following characteristics: (1) un-sufficient contact with solder surface; (2) non-wetting behavior; (3) maximum wetting force lies below Buoyance line; and (4) abnormal force evolution during the test. To evaluate the wettability, wetting time and maximum wetting forces are determined from successful tests only. The wetting time is defined as the time at which the force crosses zero value. The maximum

wetting forces were taken at measuring time of 5 s for the curves with wetting time shorter than 3 s and at 8 s for all other cases. In general, the higher the maximum wetting force or the lower the wetting time, the better wettability. The data was plotted as box chart, with standard deviation shown as error bars. In some cases, the wetting rate is referred to as the slope of wetting curves, as shown in Figure 5.

3. Results

3.1. The Comparison Between Wetting Balance Tests with Globule and Conventional Bath

Figure 6 displays the wetting force–time curves for micro-wetting tests of SAC305 and Cu strips with different immersion depths. The curves for the tests with conventional bath are also shown for comparison. One can see that the curves from the micro-wetting test fluctuate more than those from the conventional tests. The micro-wetting tests exhibit long incubation time before wetting starts, especially for the tests with immersion depth of 0.5 mm. This behavior indicates a delay in thermal transfer between globule and Cu strip during the micro-wetting tests.

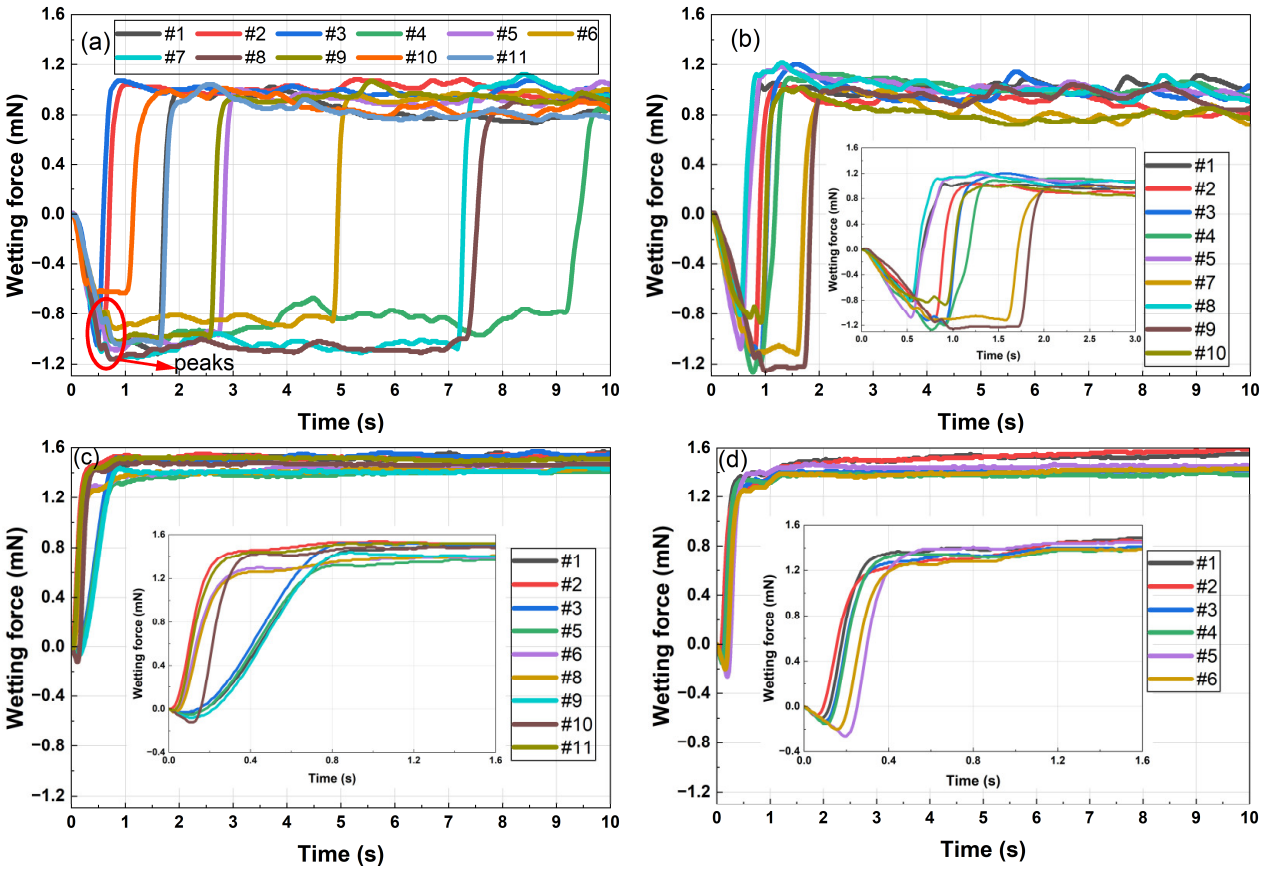

Figure 6. Wetting curves of Cu strips tested with SAC305 solder in configuration 2 at temperature of 245 °C and immersion speed of 1 mm/s for micro-wetting and conventional tests at two immersion depths: (**a**) 4 mm diameter globules, 0.5 mm-depth; (**b**) 4 mm diameter globules, 1.0 mm-depth; (**c**) bath, 0.5 mm-depth; and (**d**) bath, 1.0 mm-depth. Inserts enlarge the curves at initial period. Label #x denotes test number x.

The value of wetting time and maximum wetting forces extracted from the curves are summarized in Figure 7a. Compared to immersion depth of 1 mm, micro-wetting tests with immersion depth of 0.5 mm exhibit much larger scatter in the measured wetting time. Particularly, the wetting time is 3.98 ± 3.14 s for the micro-wetting tests with immersion depth of 0.5 mm, whereas it is 0.89 ± 0.22 s for those with immersion depth of 1.0 mm.

These values correspond to the coefficients of variation of approximately 79% and 25% for the tests with 0.5 and 1.0 mm immersion depths, respectively. The larger variability at the smaller immersion depth is primarily associated with prolonged incubation time. This fact suggests the immersion depth plays important role in heat transfer for micro-wetting tests. For the micro-wetting tests, there is a small peak in the curves within the first second, which is likely related to a change in the globule's shape due to thermal influence on properties of molten solder when immersing Cu strips into it (more detail on this effect will be discussed later).

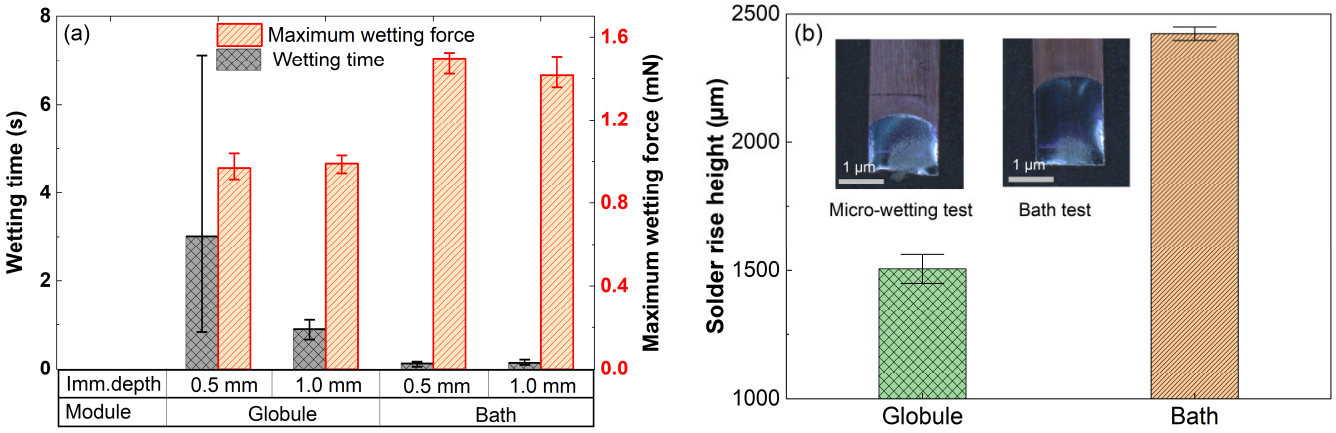

Figure 7. (**a**) Summary data of wetting time and maximum wetting forces for micro-wetting and conventional tests from the curves in Figure 6. (**b**) Solder raised height on Cu-strips for both tests in case of immersion depth of 1 mm. Error bars represent standard deviation values. Inserts are microscope images of Cu strips after the tests.

Compared to conventional tests, the maximum wetting forces are lower, and wetting times are higher for the micro-wetting tests. The results are consistent with the difference in solder rise height observed for the two test methods, as shown in Figure 7b, where the rise height in conventional tests is approximately 1.5 times higher than that in microwetting tests.

3.2. The Micro-Wetting Test for 1206 Chip Resistors

3.2.1. The Impact of the Positioning Configuration

The time–wetting force curves for the two configurations are shown in Figure 8. The wetting time and maximum wetting forces extracted from the successful curves are plotted in Figure 9. Globule sizes are 4 mm in diameter. Like the micro-testing with Cu strips described in Section 3.1, the time–wetting force curves exhibit numerous fluctuations, and the results are not reproducible for both configurations. There are numerous failed tests for both configurations. Particularly, there are 42% and 33% tests failed for configuration 1 and configuration 2, respectively. Interestingly, although the wetting times of two configurations are likely in the same range, the tests with configuration 1 exhibit slower wetting rate than those with configuration 2, as shown in Figure 8b,d. Most successful tests with configuration 2 show a long incubation time before the onset of wetting, followed by a high wetting rate. The primary difference between the configuration 1 and 2 is the metal contact area. For example, at the same immersion depth of 0.2 mm, the metal contact area is 0.3 mm^2 for configuration 1, whereas it is 1.14 mm^2 for configuration 2.

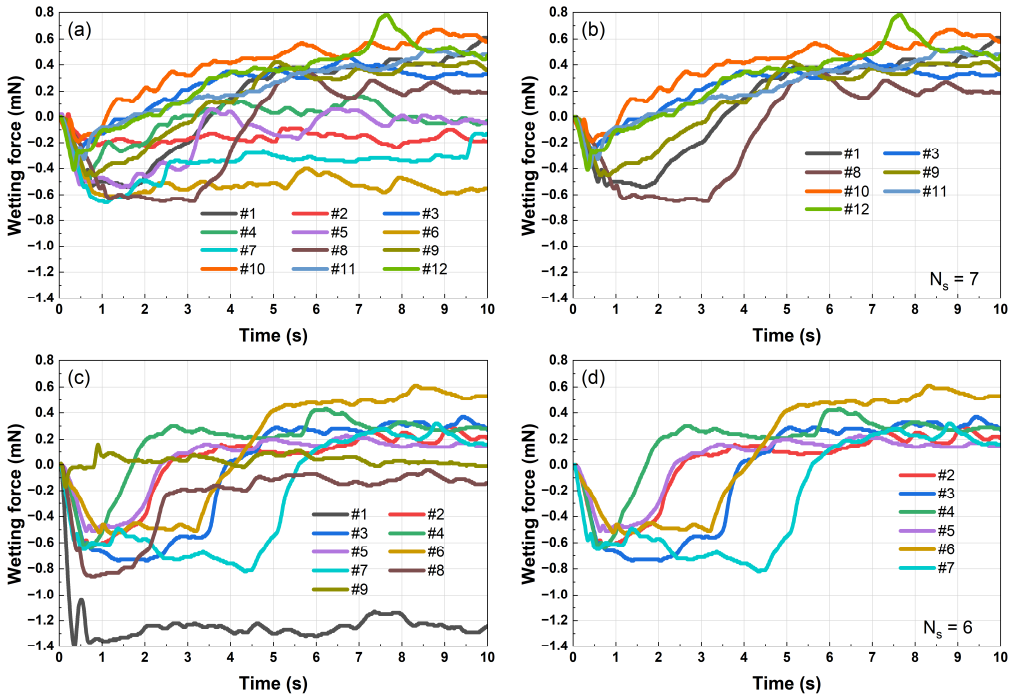

Figure 8. Wetting force curves of 1206 chip resistors tested with 4 mm diameter SAC305 globules at 245 °C with an immersion depth of 0.2 mm and a speed of 1 mm/s for the different configurations: (**a**,**b**) configuration 1 and (**c**,**d**) configuration 2. In (**b**,**d**), only wetting curves of successful tests are displayed for better visualization. Label #x denotes test number x. N_s indicates the number of successful tests.

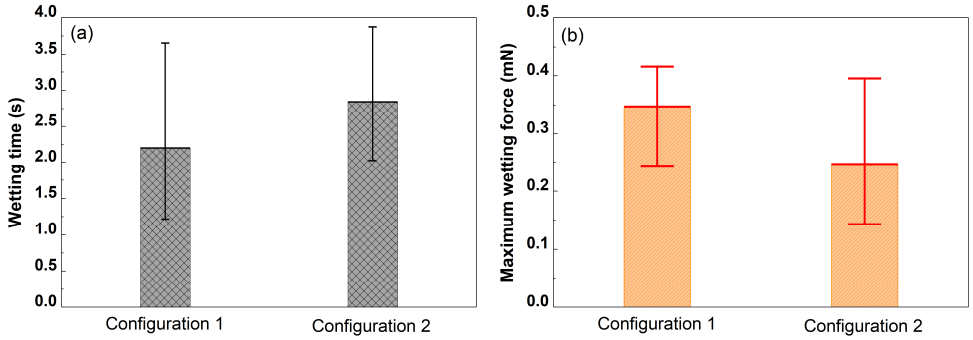

Figure 9. Wetting time (**a**) and maximum wetting forces (**b**) of 1206 chip resistors tested with 4 mm diameter SAC305 globules at 245 °C with immersion depth of 0.2 mm, immersion speed of 1 mm/s in configuration 1 and configuration 2. Data was extracted from the curves shown in Figure 8b,d. Error bars represent standard deviation values.

3.2.2. The Impact of the Immersion Depth and Speed

Changing immersion speed results in a change in immersion time. For example, lower immersion speed requires more time to reach the target depth, which might affect thermal transport between the solder and component. In this work, due to limitation of dimension of the resistors, the immersion depth varied in the range of 0.1–0.5 mm, and speed varied in the range of 0.5–1 mm/s. With these small variations, the influence of immersion depth on micro-wetting behavior is negligible. The wetting time and maximum forces are in the same range for all the tests. Figure 10 displays wetting curves of the tests conducted in configuration 1 with immersion depth of 0.2 mm and speed of 0.5 mm/s. The micro-wetting behavior is consistent with that observed for the tests with immersion speed of 1.0 mm/s, as shown in Figure 8b. One practical challenge, however, is that these tests with small immersion depths were difficult to perform. Many trials failed because the component

stopped moving as soon as it approached solder surface, preventing proper contact with the globule. It is supposed that the contact point was not properly detected. In particular, the force threshold associated with interaction with globule could not be reliably identified. As a result, the signal-to-noise ratio was insufficient for precise contact detection, especially for the tests with small components. As shown in Figure 10b, 50% of the tests were failed.

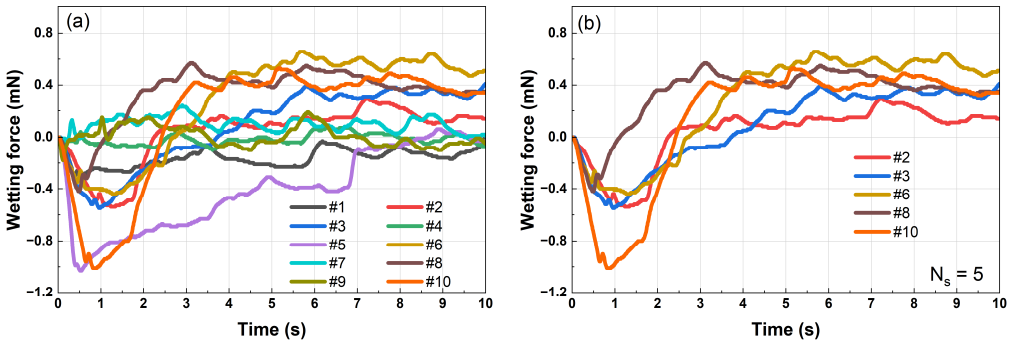

Figure 10. Wetting force curves of 1206 chip resistors tested with 4 mm-diameter SAC305 globules of configuration 1 at 245 °C with an immersion depth of 0.2 mm and a speed of 0.5 mm/s. (**a**) All tests; (**b**) only wetting curves of successful tests. Label #x denotes test number x. N_s indicates the number of successful tests.

3.2.3. The Impact of Heat Temperature and Globule Diameter

Figure 11 shows the influence of temperature and globule size on the wetting curves of 1206 chip resistors tested with SAC305 globules. One can see that the shape of the curves varies among the tests, even under same conditions. Unlike the tests with 4 mm-diameter globules at 245 °C, in which shape-change-related peaks appear in the dewetting period, for all tests with 2 mm-diameter globules or at 290 °C, these peaks disappear or appear late in the wetting period. For the tests with 4 mm-diameter globules and at 290 °C, a continuous decrease in wetting forces was observed for all successful tests, as shown in Figure 11h.

Summary data of wetting time and maximum wetting forces from the successful tests are plotted in Figure 12. Compared to tests conducted at 245 °C, lower wetting time and higher maximum wetting forces were obtained for the temperature of 290 °C, indicating better wetting behavior at this temperature. At the temperature of 245 °C, wetting times of the tests with 2 mm-diameter globules are higher than those with 4 mm-diameter globules, whereas the maximum wetting forces are likely the same for both globule diameters. In contrast, at a temperature of 290 °C, wetting times are likely the same, whereas maximum wetting forces of the tests with 2 mm-diameter globules are higher than those with 4 mm-diameter globules.

Experimental observation shows that for the tests using 2 mm diameter globules at both temperatures, the solder surface remains shiny throughout measurement, indicating that less surface oxidation occurs during the tests. This fact might be one of the reasons why fast wetting times are obtained for the tests using 2 mm-diameter globules. For the tests using 4 mm-diameter globules at 290 °C, the globules supposedly quickly oxidized, and it was very challenging to obtain a successful test. As shown in Figure 11g, 65% of the tests were failed. For the tests at 290 °C, there are some curves with two distinct bumps, such as for the tests #7, #9 in Figure 11f, and #5 and #11 in Figure 11h.

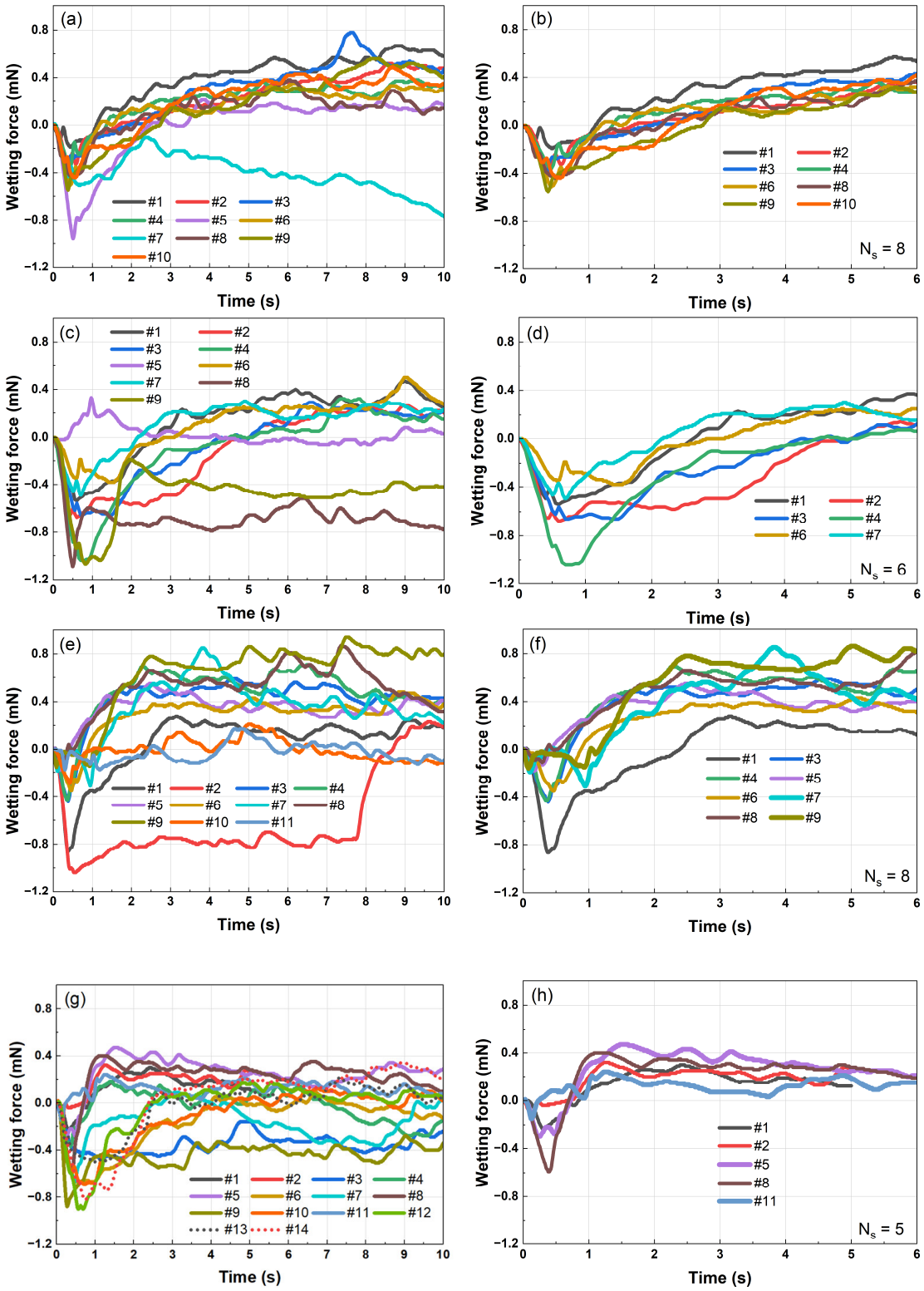

Figure 11. Wetting curves of 1206 chip resistors tested with SAC305 in configuration 1 with an immersion speed of 1 mm/s for different temperatures, globule diameters, and immersion depths. (**a**,**b**) 245 °C, 2 mm-diameter globules, and 0.2 mm depth; (**c**,**d**) 245 °C, 4 mm diameter globules, and 0.5 mm depth; (**e**,**f**) 290 °C, 2 mm-diameter globules, and 0.2 mm-depth; and (**g**,**h**) 290 °C, 4 mm-diameter globules, 0.5 mm depth. In (**b**,**d**,**f**,**h**), only wetting curves of successful tests are shown. Label #x denotes test number x. N_s indicates the number of successful tests. Thicker lines in (**f**,**h**) display curves with two distinct bumps.

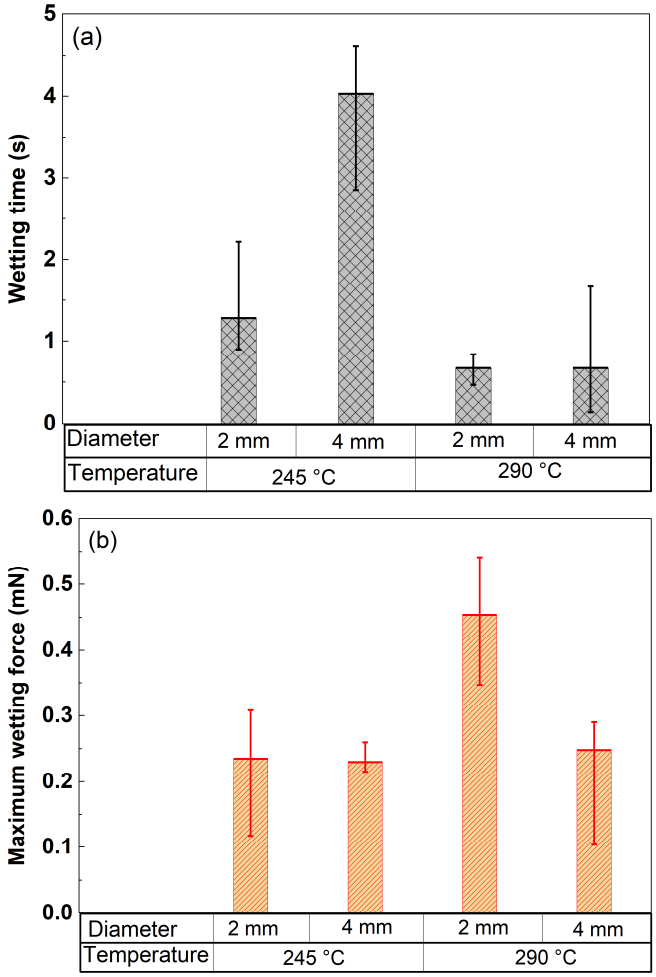

Figure 12. Wetting time (**a**) and maximum wetting forces (**b**) of 1206 chip resistors tested with SAC305 in configuration 1 with an immersion speed of 1 mm/s for different temperatures, globule diameters, and immersion depth. Data was extracted from the curves shown in Figure 11b,d,f,h. Error bars represent standard deviation values.

3.3. The Micro-Wetting Test for Chip Capacitors

3.3.1. The Impact of Globule Diameter

Figure 13 displays the wetting curves of 1206 chip capacitors tested with 2 mm- and 4 mm-diameter SAC305 globules. Compared with the tests using 4 mm-diameter globules, the tests with 2 mm diameter exhibit more uniform wetting curves, whereas for the tests using 4 mm diameter globules, micro-wetting behavior varies between experiments. Some tests exhibit a long incubation time, while others show gradual wetting that pauses temporarily before continuing. The shape-change-related peaks are observed for all the successful curves, and they appeared during dewetting period.

Compared to tests with resistors, the wetting behavior exhibits differently for the capacitor. Particularly, for the tests with 4 mm-diameter globules, many tests for capacitors have a longer incubation time than those of resistors. More tests for capacitors show a pause during wetting before a sharp increase in wetting rate, while for resistors the wetting increases gradually, as shown in Figure 11b,d. It is worth noting that capacitors have better thermal contact with globules than resistors due to a larger metal contact area.

Figure 14 shows the wetting times and maximum wetting forces of 1206 chip capacitors tested with 2 mm- and 4 mm-diameter SAC305 globules. The tests with 2 mm-diameter globules exhibit higher maximum wetting force and lower wetting time, indicating better wetting behavior for these tests.

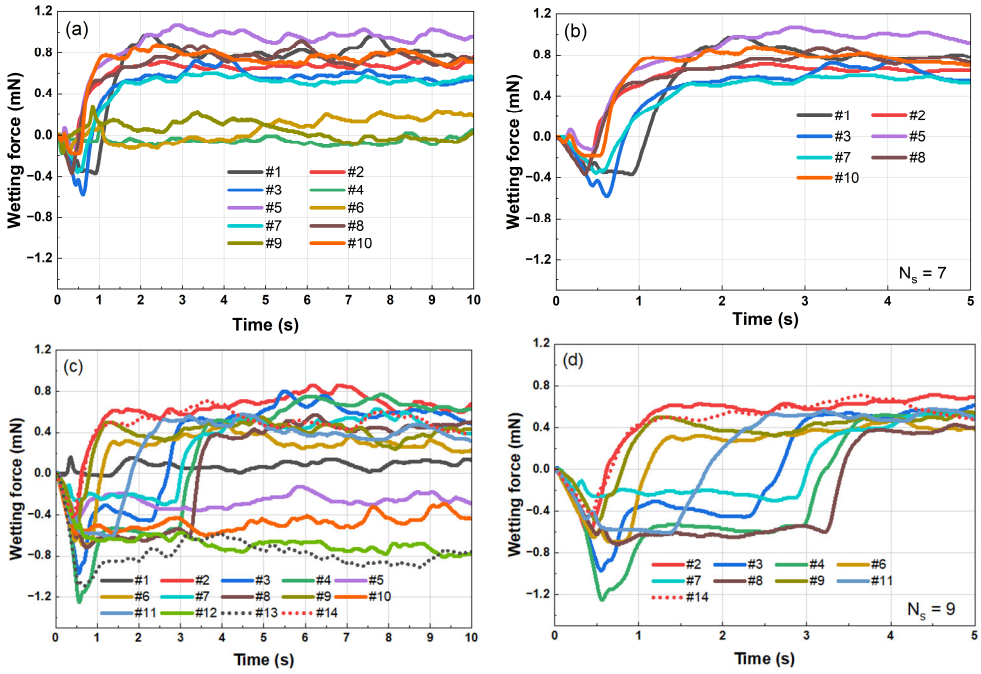

Figure 13. Wetting curves of 1206 chip capacitors tested with SAC305 at 245 °C, in configuration 1, immersion speed of 1 mm/s for different globule diameters and immersion depth. (**a**,**b**) 2 mm-diameter globules and 0.2 mm depth; (**c**,**d**) 4 mm-diameter globules and 0.5 mm depth. In (**b**,**d**) only wetting curves of successful tests are shown. Label #x denotes test number x. N_s indicates the number of successful tests.

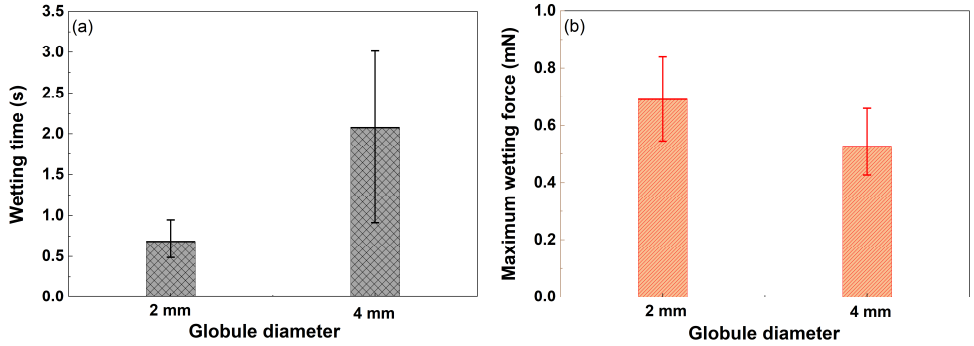

Figure 14. Wetting time (**a**) and maximum wetting force (**b**) of 1206 chip capacitor tested with SAC305 in configuration 1, immersion speed of 1 mm/s for different globule diameters and immersion depths. Data was extracted from the curves shown in Figure 13b,d. Error bars represent standard deviation values.

3.3.2. The Micro-Wetting Tests for 0603 Chip Capacitors

Figure 15 plots the wetting curves of micro-wetting tests with 0603 capacitors at temperatures of 245 and 290 °C. The 2 mm-diameter globules were used. The use of 4 mm-diameter globules was challenging due to practical difficulty during positioning steps. In particular, achieving proper contact is challenging due to the difficulty of aligning the component edge with the pole of the globule (see configuration 1, Figure 4a). As seen in Figure 15b, some curves exhibit two distinct bumps during wetting stages (see #3 and #7). Since the immersion time for these tests is only 0.2 s, it is supposed that the second bump is not a result from a second dewetting process but from a rearrangement of acting forces on the components, which is related change in globule's shape, or thermal transport between globule and components. The summarized data of wetting time and maximum wetting forces of the tests for 0603 chip capacitors are shown Figure 16. The results from 1206 chip

capacitors are also shown for comparison. One can see that the wetting behavior is better at temperature of 290 °C with higher maximum wetting forces and shorter wetting time. Compared to 1206 capacitors, the tests on 0603 capacitors have slightly higher wetting time but lower wetting forces. It is reasonable since the 1206 capacitor has larger size and therefore interacts with a greater volume of solder.

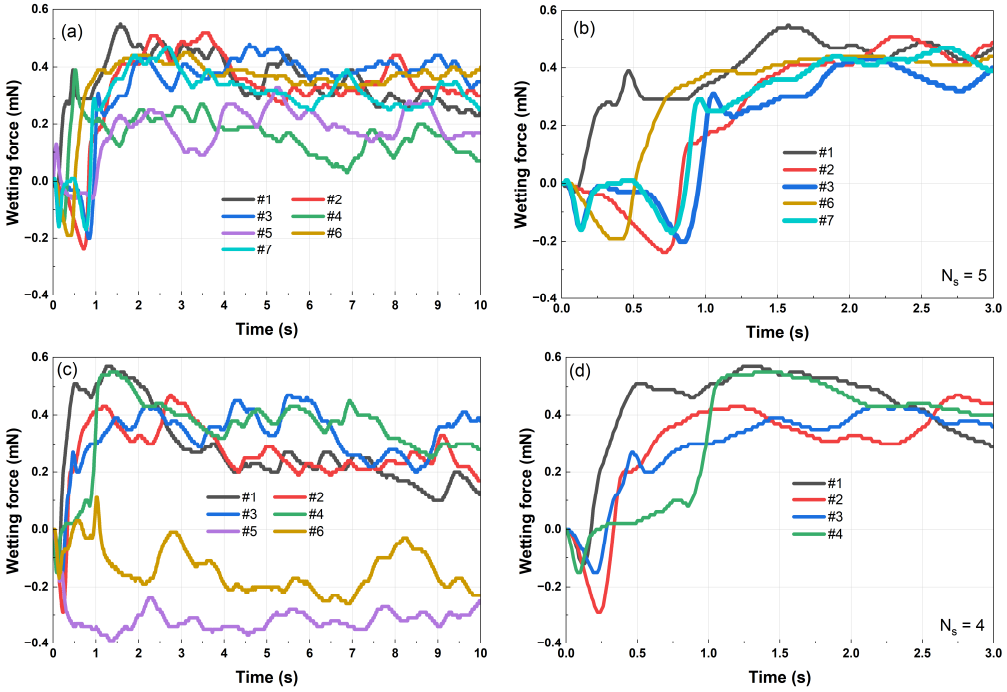

Figure 15. Wetting curves of 0603 chip capacitors tested with 2 mm-diameter SAC305 in configuration 1 with an immersion speed of 1 mm/s, immersion depth of 0.2 mm, and a temperature of (**a**,**b**) 245 °C and (**c**,**d**) 290 °C. In (**b**,**d**) only wetting curves of successful tests are shown. Label #x denotes test number x. N_s indicates the number of successful tests. Thicker lines in (**b**) display curves with two distinct bumps.

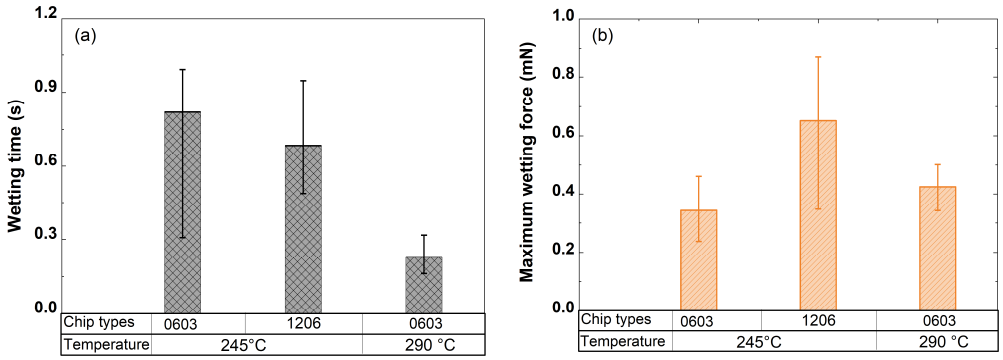

Figure 16. Wetting time (**a**) and maximum wetting force (**b**) of 0603 chip capacitors tested with 2 mm-diameter SAC305 in configuration 1, immersion speed of 1 mm/s, immersion depth of 0.2 mm, and at temperatures of 245 and 290 °C. Data was extracted from the curves in Figure 15b,d. Data for 1206 chip capacitors was taken from Figure 14 for the tests using 2 mm-diameter globules.

3.4. The Micro-Wetting Behavior of SnBi58

Figure 17 presents the wetting curves of 1206 chip capacitors tested with SnBi58 solder. The wetting curves look similar to those of the tests with SAC305 solder (see Figure 13c,d), including strong fluctuations, slow wetting rate, or noticeable pause in wetting process. The wetting times are slightly lower compared to tests with SAC305, but the maximum wetting forces of the tests using SnBi58 solder are much lower, typically only about one-third of

the forces measured for the tests using SAC305 solder, as shown in Figure 18. Observation indicates that unlike the 4 mm-diameter SAC305 globules, the surface of SnBi58 globules remained shiny during the tests, indicating the effect of surface oxidation of solder can be subtracted from the tests. In general, SnBi58 has lower surface tension and higher contact angle than SAC305 [15], resulting in lower wetting forces.

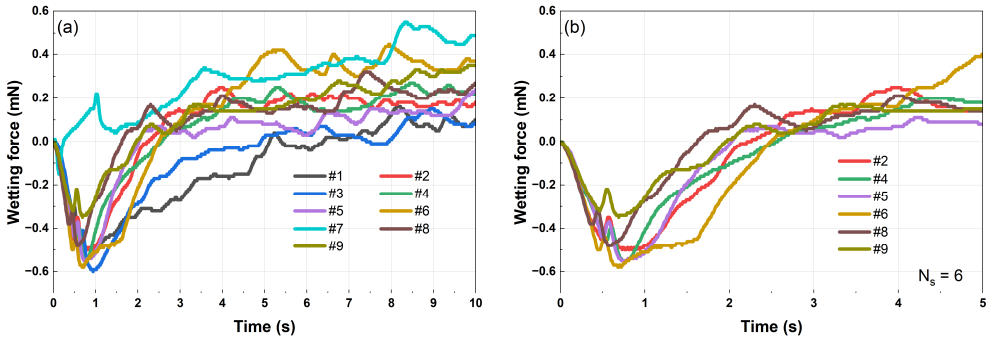

Figure 17. Wetting curves of 1206 chip capacitors tested with 4 mm-diameter SnBi58 in configuration 1, immersion depth of 0.5 mm, immersion speed of 1 mm/s, and temperature of 160 °C. (**a**) All tests; (**b**) only wetting curves of successful tests are shown. Label #x denotes test number x. N_s indicates the number of successful tests.

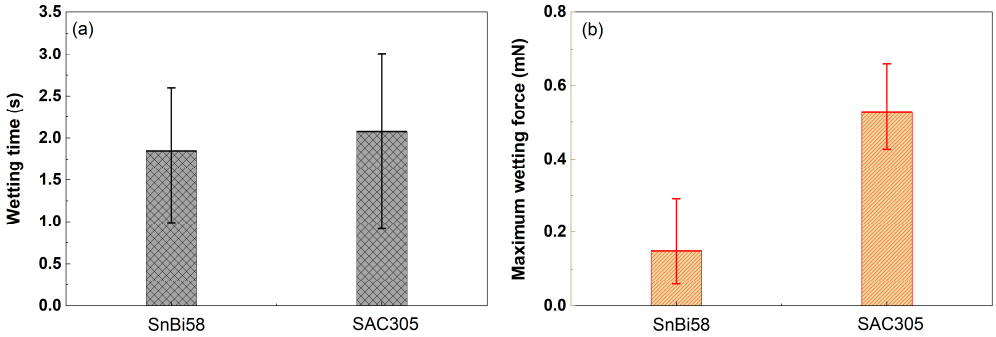

Figure 18. Wetting time (**a**) and maximum wetting force (**b**) for micro-wetting tests of 1206 chip capacitors with SnBi58. Data was extracted from Figure 17b. The results for micro-wetting tests with 4 mm diameter SAC305 globules at 245 °C, which is displayed in Figure 14, are shown for comparison. All tests were performed with configuration 1, immersion depth of 0.5 mm, immersion speed of 1 mm/s. Error bars represent standard deviation values.

4. Discussion

4.1. Difference in Heat Transfer Between Micro-Wetting and Conventional Tests

Compared to conventional bath tests, the wetting times are higher, and the measured wetting forces are lower for micro-wetting tests (see in Figure 7). The reason for the difference in wetting behavior could be attributed to two factors: (1) Solder surface oxidation: in micro-wetting tests, the globules supposedly quicky oxidized and not cleaned right before measuring, whereas in conventional tests, the surface was cleaned before measuring; (2) thermal transfer losses: due to different thermal mass between globule and bath, there is different thermal transfer between Cu and solder. The conventional test with larger bath volume ensures more uniform and stable heat transfer, whereas the Cu strip tends to rapidly cool the globules when they come to contact. The difference in thermal distribution within the solder-Cu strip system alters the surface tension and flux activation, consequently, affects the wetting behavior. To provide a rough estimation of this thermal cooling effect, the heat transfer between solder and Cu was estimated using the lumped thermal model. The following assumptions are considered: (1) the globule is considered to have uniform

temperature distribution; (2) the Cu strip acts as an infinite heat sink; (3) the continuous heating and convection in the real system is neglected. The time-dependent temperature of the globule is estimated as follows [37,38]:

$$T(t) = T_{Cu\_i} + (T_{G\_i} - T_{Cu\_i}) * \exp\left(-\frac{t * h * A}{m_G * C_G}\right)$$

where T_{Cu_i} and T_{G_i} are the initial temperatures of Cu strip and globule, and m_G and C_G are the mass and specific heat of the solder. A is contact area, and h is the contact heat transfer coefficient. The specific heat capacity of SAC is taken as 220.7 J/(kg·K) [39], and h is taken as a time-dependent function for the liquid/solid interface of SnCu0.7 solder on Cu substrate as reported in the literature [40].

Figure 19 plots the time-dependent temperatures of the globule and bath after contacting with Cu strip at immersion depths of 0.5 and 1 mm. As expected, the temperature of the bath remains unchanged, whereas the temperature of the globule decreases rapidly. For example, after 1 s a decrease in temperature of approximately 100 °C can be observed for the globule with immersion depth of 1.0 mm. It is important to note that this model provides a rough estimation of the cooling effect and does not reflect the reality of the micro-wetting tests, because (A) the heating module is continuously heating the globule; (B) the contact area A is not constant, and it will start with the bottom area of the Cu specimen and grow by the addition of the wetted lateral area of the specimens; and (C) Molten solder is liquid, which induces convection heat transfer within the globule. The optimum immersion depth should minimize the cooling effect while still ensuring sufficient thermal contact to achieve rapid thermal equilibrium. The micro-wetting tests with an immersion depth of 1.0 mm show better wetting behavior than those with immersion depth of 0.5 mm (see Figure 7), indicating that the deeper immersion enhances thermal contact and promotes wettability of solder.

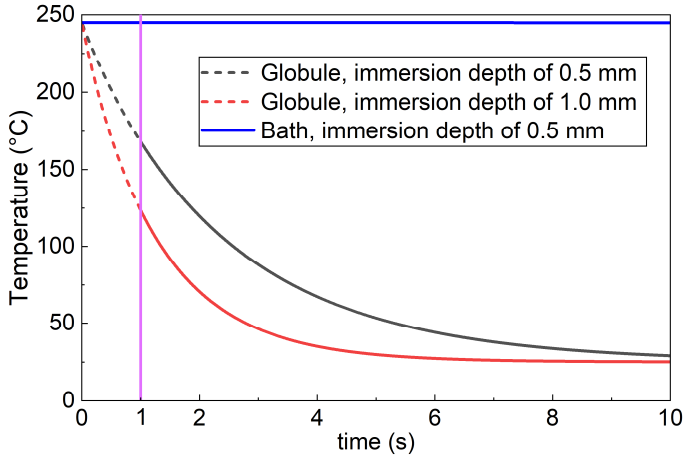

Figure 19. Estimated temperature of 4 mm-diameter SAC globule as function of time with immersion depth of 0.5 and 1.0 mm. The estimated value for bath with immersion depth of 0.5 mm is drawn as the blue one. Dash lines describe the estimated temperature in the first second. The purple line is shown as intersection at time = 1 s for visualization purpose.

4.2. Micro-Wetting Behavior

Wetting behavior is influenced by several interacting processes, including thermal transfer, flux activation, and surface condition of both component and solder. Changes to any of these factors directly alters wetting behavior. Especially for small solder volume, the ideal thermal management between solder and components is a result of compromise between the contact area (like in the case of different immersion depth and positioning

configurations), the globule size, and the initial temperature. High temperature and small globule diameter are the best choice for micro-wetting tests. They enhance better thermal transfer and minimize the influence of surface oxidation. For example, the difference in behavior between the tests with 2 mm- and 4 mm-diameter globules can be attributed to the larger thermal mass and slower heat transfer associated with the 4 mm globules. The thermal management involves heat transfer among the heating module, the globules, and the component. It is supposed that more time is needed for bigger globules to reach thermal equilibrium, and that the onset of wetting becomes more sensitive to small variations in initial temperature, immersion conditions, and local solder flow. As a result, some tests show prolonged incubation, while others begin wetting gradually but momentarily stay still when the temperature or interfacial conditions are not yet favorable for continuous spreading (see Figures 11 and 13). In addition, the larger surface area of the 4 mm globules enhances the influence of surface irregularities or oxide layers. Even slight differences in oxide thickness or distribution can locally inhibit wetting, causing the observed pauses or delays. For the smaller 2 mm globules, these effects are less pronounced. It is because better thermal management and less surface area allow the interface to heat more uniformly and the oxide layer—if present—to break more consistently, leading to more repeatable and shorter incubation times.

For small globules, minor movements of the solder and changes in surface tension can result in change in its shape. The instability of solder shape causes wetting curve fluctuations as well as abnormal signals in the curves, such as the small peaks observed in almost all tests. Particularly, the shape changes may momentarily alter the balance of forces acting on the molten solder, leading to a brief fluctuation in the measured signal. Slight adjustments in the globule's curvature or surface profile can modify the local wetting dynamics, resulting in a transient increase in force or displacement. Such effects might be more pronounced at lower temperatures, where the viscosity and surface tension of the solder are higher, making the globule less responsive to deformation. At elevated temperatures, the solder becomes more fluid, allowing the globule to stabilize more quickly, which explains why the peak diminishes or disappears in the 290 °C tests. A similar explanation can be applied for the micro-wetting tests with 4 mm-diameter globules. Because of larger thermal mass, the required time to reach thermal equilibrium for these tests is longer compared to that of 2 mm-diameter globules. This delay might increase the sensitivity of the wetting response to small variations in temperature and interfacial conditions, promoting the observed peak behavior.

The shape-change-related peaks also appear in the wetting curves for tests with chip capacitors, but primarily before wetting onset (see Figure 10). It might be related to the fact that at the same immersion depth, the metal contact area of capacitor is larger than that of the resistor (see Figure 2b,c). Additionally, mechanical interactions during immersion—such as minor misalignment of the substrate or variations in immersion speed—may also influence the onset or magnitude of this peak. However, the consistent temperature and globule size dependence observed across tests suggests that thermophysical properties of the solder, rather than experimental artifacts, are the primary cause.

In summary, there are four possible factors may contribute to the appearance of the small peaks: (1) thermal imbalance, (2) surface oxidation, (3) mechanical misalignment, and (4) instability of globule shape. In future work, further analysis combining high-speed imaging and numerical modeling will be conducted to confirm the exact mechanism and quantify how globule shape transitions influence the wetting force response.

4.3. Applicability of Micro-Wetting Tests

Micro-wetting tests have demonstrated a strong capability to evaluate the wetting behavior of molten solders under conditions closer to the actual soldering process than conventional baths. The tests allow measuring wetting time, maximum wetting forces, and capturing the dynamic evolution of wetting behavior as thermal and surface condition changes. For example, the improvement in wetting behavior at a temperature of 290 °C with 2 mm-diameter globules is reasonable, due to better thermal transfer between component and solder and suppression of surface oxidation, respectively. Importantly, micro-wetting tests enable to capture the wetting behavior of low melting point SnBi58 solder on chip components, highlighting its potential as a promising method to assessment solderability toward miniaturization of electronics.

4.4. Limitation of the Test-Link to Standards

One challenge for micro-wetting tests is how to evaluate the solder wettability via the parameters extracted from the wetting curves. In general, wetting time and maximum wetting force are two key indicators for the wetting behavior of a solder [15,31]. In some cases, the wetting rate or tangent to wetting curve has also been taken into account [41]. In this work, the results were compared to the IPC J-STD-002 [35] standard, which defines a test as passing when wetting time is less than 1 s, and measured wetting forces at 2 and 5 s are equal or higher than the specified threshold values.

For the micro-wetting test with Cu strips, only 30% of the tests with immersion depth of 1 mm satisfy the IPC J-STD-002 criteria. For the tests with chip resistors and capacitors, most tests failed the standard since the measured wetting times exceeded 1 s. In some cases, particularly those using 2 mm-diameter globules, the wetting time was less than 1 s (see Figure 16a). Nevertheless, these tests still failed to satisfy the standard because the wetting forces measured at 2 and 5 s did not reach the specified threshold values. However, to properly evaluate overall wettability and enable meaningful comparison to standard reference values, the maximum force associated with the dimensions of both the globule and component should be considered. The influence of instability of the globular shape on the wetting curve should be subtracted for precise interpretation on the wetting behavior. Overall, the results indicate that applying conventional IPC J-STD-002 acceptance criteria directly to micro-wetting tests may be overly conservative. The observed sensitivity of wetting force to globule size and shape stability suggests that acceptance thresholds may need to be scaled with solder volume and component dimensions when micro-wetting methods are used. Rather than serving as a direct pass–fail replacement, micro-wetting tests could inform adjusted or supplementary acceptance criteria—such as normalized wetting force or corrected wetting curves—that better reflect intrinsic wettability while remaining consistent with established industry standards.

5. Conclusions

This work aims to make a comprehensive study on the wetting behavior of SAC305 and SnBi58 solders on chip components using the micro-wetting balance method. The results have demonstrated that the micro-wetting test is an effective method to evaluate solder wettability under conditions that are closer to the actual soldering process than conventional wetting balance tests using a bath. Thermal transfer between solder and components and surface condition plays significant role in determining the overall wetting performance. Despite fluctuation in the wetting curves, micro-wetting tests successfully capture the key wetting characteristics for both SAC305 and SnBi58 solder, underscoring its potential as a reliable assessment method for solderability toward miniaturization. Overall, the following keys conclusions can be drawn:

- Compared to conventional bath tests, micro-wetting tests exhibit higher wetting time and lower maximum wetting forces. The wetting curves obtained from micro-wetting tests fluctuate more than the curves from conventional tests. In addition, the solder rise height is higher in the micro-wetting tests.
- The component-positioning configuration has significant influence on the wetting rate of solder on chip components. The tests conducted in vertical configuration show longer wetting rate than those in the horizontal configuration, whereas the wetting curves of the tests conducted in horizontal configuration exhibit longer incubation time.
- In the case of micro-wetting tests for chip components, higher temperatures and smaller globule sizes provides (A) better thermal management between solder and components and (B) reduced solder surface oxidation. As a result, lower wetting times were achieved.
- The micro-wetting tests enable solderability evaluation for small components (0603 chip capacitors), as small globules are used. For this component, wetting times are smaller than 1 s for all the tests.
- Compared with tests using SAC305 solder, the tests using SnBi58 show similar wetting time, but significantly lower the maximum wetting forces. The maximum forces obtained for the tests using SnBi58 are approximately one third of those obtained for the tests using SAC305.
- Micro-wetting tests for chip components failed to satisfy the IPC J-STD-002 standard. The acceptance thresholds may need to be scaled with solder volume and component dimensions when micro-wetting methods are used.

Author Contributions: Conceptualization, C.T.T. and S.W.; methodology, C.T.T. and S.W.; software, C.T.T.; investigation, C.T.T.; writing—original draft, C.T.T.; writing—review and editing, C.T.T. and S.W.; supervision, C.T.T. and S.W. All authors have read and agreed to the published version of the manuscript.

Funding: This research received no external funding.

Institutional Review Board Statement: Not applicable.

Informed Consent Statement: Not applicable.

Data Availability Statement: The original contributions presented in this study are included in the article. Further inquiries can be directed to the corresponding author.

Acknowledgments: The authors would like to offer particular thanks to A. Ruh for his support in preparation of SnBi58 globules for micro-wetting tests and microscope images of specimens; to E. Wiss, S.-G. Anthati, and D. Barth for their support with pictures of the test; and to E. Wiss for his valuable advice.

Conflicts of Interest: The authors declare no conflicts of interest.

References

1. Niemann, J.; Härter, S.; Kästle, C.; Franke, J. Challenges of the Miniaturization in the Electronics Production on the example of 01005 Components. In *Tagungsband des 2. Kongresses Montage Handhabung Industrieroboter*; Schüppstuhl, T., Franke, J., Tracht, K., Eds.; Springer: Berlin/Heidelberg, Germany, 2017; pp. 113–123.
2. Dele-Afolabi, T.T.; Ansari, M.N.M.; Azmah Hanim, M.A.; Oyekanmi, A.A.; Ojo-Kupoluyi, O.J.; Atiqah, A. Recent Advances in Sn-Based Lead-Free Solder Interconnects for Microelectronics Packaging: Materials and Technologies. *J. Mater. Res. Technol.* **2023**, *25*, 4231–4263. [CrossRef]
3. Choudhury, S.F.; Ladani, L. Miniaturization of Micro-Solder Bumps and Effect of IMC on Stress Distribution. *J. Electron. Mater.* **2016**, *45*, 3683–3694. [CrossRef]

4. Lee, N.-C. Future Lead-Free Solder Alloys and Fluxes—Meeting Challenges of Miniaturization. In Proceedings of the 2008 10th Electronics Packaging Technology Conference, Singapore, 9–12 December 2008; pp. 864–872.
5. Josell, D.; Wallace, W.E.; Warren, J.A.; Wheeler, D.; Powell, A.C. Misaligned Flip-Chip Solder Joints: Prediction and Experimental Determination of Force-Displacement Curves. *J. Electron. Packag.* **2002**, *124*, 227–233. [CrossRef]
6. Pan, K.; Ha, J.H.; Wang, H.; Xu, J.; Park, S. An Analysis of Solder Joint Formation and Self-Alignment of Chip Capacitors. *IEEE Trans. Compon. Packag. Manuf. Technol.* **2021**, *11*, 161–168. [CrossRef]
7. Zhang, P.; Xue, S.; Wang, J. New Challenges of Miniaturization of Electronic Devices: Electromigration and Thermomigration in Lead-Free Solder Joints. *Mater. Des.* **2020**, *192*, 108726. [CrossRef]
8. Chen, C.; Tong, H.M.; Tu, K.N. Electromigration and Thermomigration in Pb-Free Flip-Chip Solder Joints. *Annu. Rev. Mater. Res.* **2010**, *40*, 531–555. [CrossRef]
9. Wang, D.; Ling, H.; Sun, M.; Miao, X.; Hu, A.; Li, M.; Dai, F.; Zhang, W.; Cao, L. Investigation of Intermetallic Compound and Voids Growth in Fine-Pitch Sn–3.5Ag/Ni/Cu Microbumps. *J. Mater. Sci. Mater. Electron.* **2018**, *29*, 1861–1867. [CrossRef]
10. Yang, W.-R.; Yasuda, K.; Song, J.-M. Mechanical Properties of Intermetallic Compounds at Solder Joint Interfaces Investigated Using Nanoindentation Technique. *J. Adv. Join. Process.* **2025**, *12*, 100356. [CrossRef]
11. Vijay, K. Miniaturization—Solder Paste Attributes for Maximizing the Print & Reflow Manufacturing Process Window. In Proceedings of the 2012 4th Electronic System-Integration Technology Conference, Amsterdam, The Netherlands, 17–20 September 2012; pp. 1–13.
12. Illés, B.; Géczy, A.; Tafferner, Z.; Skwarek, A.; Krammer, O. Low-Temperature Soldering (LTS) in the Electronics Industry: A Brief Review. In Proceedings of the 2025 International Spring Seminar on Electronics Technology (ISSE), Budapest, Hungary, 14–18 May 2025; pp. 1–6.
13. Lee, B.-H.; Chang, C.-Y.; Li, C.-H.; Lin, K.-S.; Yueh, S.-L.; Kobayashi, S. New-Generation, Low-Temperature Lead-Free Solder for SMT Assembly. In Proceedings of the SMTA Proceedings, Rosemont, IL, USA, 14–18 October 2018.
14. Huang, B.; Dasgupta, A.; Lee, N.-C. Effect of SAC Composition on Soldering Performance. In Proceedings of the IEEE/CPMT/SEMI 29th International Electronics Manufacturing Technology Symposium, San Jose, CA, USA, 14–16 July 2004; pp. 45–55.
15. Jung, D.-H.; Jung, J.-P. Review of the Wettability of Solder with a Wetting Balance Test for Recent Advanced Microelectronic Packaging. *Crit. Rev. Solid State Mater. Sci.* **2019**, *44*, 324–343. [CrossRef]
16. Králová, I.; Pilnaj, D.; Pop-Georgievski, O.; Uřičář, J.; Veselý, P.; Klimtová, M.; Dušek, K. Wettability in Lead-Free Soldering: Effect of Plasma Treatment in Dependence on Flux Type. *Appl. Surf. Sci.* **2024**, *668*, 160447. [CrossRef]
17. Li, Q.; Li, Z.; Yan, H.; Ren, Z.; Li, C.; Liu, A.; Pang, W.; Ren, G.; Liao, M.; Zhang, R.; et al. Current Status on Optimizing Solder Wettability from Substrate Surface Treatment, Alloying Solder, Flux, and Process Environments. *Mater. Sci. Semicond. Process.* **2025**, *200*, 109978. [CrossRef]
18. Dušek, K.; Novák, M.; Mach, P. Solderability Measurement of Copper with Different Surface Finishes. In Proceedings of the 33rd International Spring Seminar on Electronics Technology, ISSE 2010, Warsaw, Poland, 12–16 May 2010; pp. 113–116.
19. Lopez, E.P.; Vianco, P.T.; Rejent, J.A. Solderability Testing of Sn-Ag-XCu Pb-Free Solders on Copper and Au-Ni-Plated Kovar Substrates. *J. Electron. Mater.* **2005**, *34*, 299–310. [CrossRef]
20. Bušek, D.; Plaček, M.; Růžička, D. Wetting Balance Test—Comparison of Solder Alloys Wetting. In Proceedings of the 2017 40th International Spring Seminar on Electronics Technology (ISSE), Sofia, Bulgaria, 10–14 May 2017; pp. 1–5.
21. Rizvi, M.J.; Chan, Y.C.; Bailey, C.; Lu, H.; Islam, M.N.; Wu, B.Y. Wetting and Reaction of Sn-2.8Ag-0.5Cu-1.0Bi Solder with Cu and Ni Substrates. *J. Electron. Mater.* **2005**, *34*, 1115–1122. [CrossRef]
22. Abtew, M.; Selvaduray, G. Lead-Free Solders in Microelectronics. *Mater. Sci. Eng. R Rep.* **2000**, *27*, 95–141. [CrossRef]
23. Gunter, I.A. The Solderability Testing of Surface Mount Devices Using the GEC Meniscograph Solderability Tester. *Circuit World* **1986**, *13*, 8–12. [CrossRef]
24. Whalley, D.C.; Conway, P.P. Simulation and Interpretation of Wetting Balance Tests Using the Surface Evolver. *J. Electron. Packag.* **1996**, *118*, 134–141. [CrossRef]
25. Lea, C. Quantitative Solderability Measurement of Electronic Components—Part I. *Solder. Surf. Mt. Technol.* **1990**, *2*, 8–13. [CrossRef]
26. Klabacka, E.; Urbanek, J. A Note on Some Limitations in the Wetting-Balance Measurements and How to Deal with Them. In Proceedings of the 2006 International Conference on Applied Electronics, Pilsen, Czech Republic, 6–7 September 2006; pp. 93–95.
27. Sargent, P.M.; Tang, A.C.T.; Gordon, F.H. An Experimental Study of the Variation of Wettability of SMDs Using the Micro-Globule Wetting Method. In Proceedings of the [1991 Proceedings] Eleventh IEEE/CHMT International Electronics Manufacturing Technology Symposium, San Francisco, CA, USA, 16–18 September 1991; pp. 166–170.
28. Conway, P.P. Solderability Testing of Alternate Component Termination Materials with Lead Free Solder Alloys. In Proceedings of the Seventeenth IEEE/CPMT International Electronics Manufacturing Technology Symposium. "Manufacturing Technologies—Present and Future", Austin, TX, USA, 2–4 October 1995; pp. 245–251.

29. Tseng, C.-F.; Duh, J.-G. Correlation between Microstructure Evolution and Mechanical Strength in the Sn–3.0Ag–0.5Cu/ENEPIG Solder Joint. *Mater. Sci. Eng. A* **2013**, *580*, 169–174. [CrossRef]
30. Phoosekieaw, P.; Khunkhao, S. A Study of Several Board Finish Solderability with Sn-Ag-Cu under Different Atmospheres. In Proceedings of the 2012 9th International Conference on Electrical Engineering/Electronics, Computer, Telecommunications and Information Technology, Phetchaburi, Thailand, 16–18 May 2012; pp. 1–4.
31. Ramli, M.I.I.; Mohd Salleh, M.A.A.; Abdullah, M.M.A.; Narayanan, P.; Chaiprapa, J.; Mohd Said, R.; Yoriya, S.; Nogita, K. The Effect of Ni and Bi Additions on the Solderability of Sn-0.7Cu Solder Coatings. *J. Electron. Mater.* **2020**, *49*, 1–12. [CrossRef]
32. Ramli, M.I.I.; Mohd Salleh, M.A.A.; Mohd Sobri, F.A.; Narayanan, P.; Sweatman, K.; Nogita, K. Relationship between Free Solder Thickness to the Solderability of Sn–0.7Cu–0.05Ni Solder Coating during Soldering. *J. Mater. Sci. Mater. Electron.* **2019**, *30*, 3669–3677. [CrossRef]
33. Moyer, J.; Zhang, W. Solder Wetting Measurement of Back Contact Paste Using a Wetting Balance. In Proceedings of the 2009 34th IEEE Photovoltaic Specialists Conference (PVSC), Philadelphia, PA, USA, 7–12 June2009; pp. 001838–001841.
34. *IEC 60068-2-20:2021*; Environmental Testing—Part 2-20: Tests—Tests Ta and Tb: Test Methods for Solderability and Resistance to Soldering Heat of Devices with Leads. International Electrotechnical Commission (IEC): Geneva, Switzerland, 2021.
35. *IPC J-STD-002D*; Solderability Tests for Component Leads, Terminations, Lugs, Terminals and Wires. IPC: Northbrook, IL, USA, 2011.
36. *IPC J-STD-003B*; Solderability Tests for Printed Boards. IPC: Northbrook, IL, USA, 2003.
37. Bejan, A. *Convection Heat Transfer*, 1st ed.; Wiley: Hoboken, NJ, USA, 2013.
38. Arumugam, A.; Buonomo, B.; Luiso, M.; Manca, O. Lumped Capacitance Thermal Modelling Approaches for Different Cylindrical Batteries. *Int. J. Energy Prod. Manag.* **2023**, *8*, 201–210. [CrossRef]
39. Bilek, J.; Atkinson, J.; Wakeham, W. Thermal Conductivity of Molten Lead-Free Solders. *Int. J. Thermophys.* **2006**, *27*, 92–102. [CrossRef]
40. Silva, B.L.; Cheung, N.; Garcia, A.; Spinelli, J.E. Evaluation of Solder/Substrate Thermal Conductance and Wetting Angle of Sn–0.7 wt%Cu–(0–0.1 wt%Ni) Solder Alloys. *Mater. Lett.* **2015**, *142*, 163–167. [CrossRef]
41. Lopez, E.; Vianco, P.; Rejent, J. Solderability Testing of 95.5Sn-3.9Ag-0.6Cu Solder on Oxygen-Free High-Conductivity Copper and Au-Ni-Plated Kovar. *J. Electron. Mater.* **2003**, *32*, 254–260. [CrossRef]